Modeling the Electrical Characteristics of Schottky Contacts in Low-Dimensional Heterostructure Devices

Regiane Ragi, Murilo Araujo Romero, and Bahram Nabet, *Member, IEEE*

***Abstract*—This paper deals with the modeling of the electronic characteristics of semiconductor devices based on Schottky contacts in low-dimensional systems. For the capacitance–voltage characteristics, a quasi-two-dimensional quantum mechanical model is developed and validated. For the current–voltage characteristics, a unified model is presented, considering both the tunneling as well as the thermionic emission mechanisms. Our theoretical predictions suggest that for photodetection applications the use of these contacts, replacing conventional metal-semiconductor junctions, can reduce the dark current by at least one order of magnitude.**

***Index Terms*—Quantum-effect semiconductor devices, Schottky barriers, semiconductor device modeling, semiconductor–metal interfaces.**

I. Introduction

THE properties of electrons in an inversion layer have attracted interest since the invention of the field-effect transistor. Further attention has been motivated by the enhanced transport properties of the two-dimensional (2-D) electron gas (2-DEG) formed at modulation doped heterointerfaces, where the inversion layer is quantized in the growth direction. Already in the early 1990s high electron-mobility transistors (HEMTs) based on this principle displayed power amplification well above 100 GHz with outstanding noise performance.

Here, we focus on the electrical characteristics of Schottky contacts in low-dimensional systems, where electronic and optical properties may differ considerably from the usual contacts with bulk semiconductors. The interface of particular interest for this paper (Fig. 1) is a Schottky contact between a three-dimensional (3-D) metal and a 2-DEG, arising from an $Al_xGa_{1-x}As$–GaAs modulation doped heterostructure grown on top of a GaAs substrate, the same layer structure of an HEMT transistor. Other configurations, beyond the scope of this paper, are also possible, including the contact between a quantum wire one-dimensional (1-D) electron gas (1-DEG) and a three-dimensional (3-D) Schottky metal [1].

In fact, since their first proposal [2], devices relying on the contact of a Schottky metal to a low-dimensional system displayed several attractive features, such as low capacitance due to the small effective cross section, excellent noise and transport characteristics due to the 2-D electron gas as well as a high breakdown voltage, making them very promising for applications in ultrahigh-frequency and low-power electronics [3].

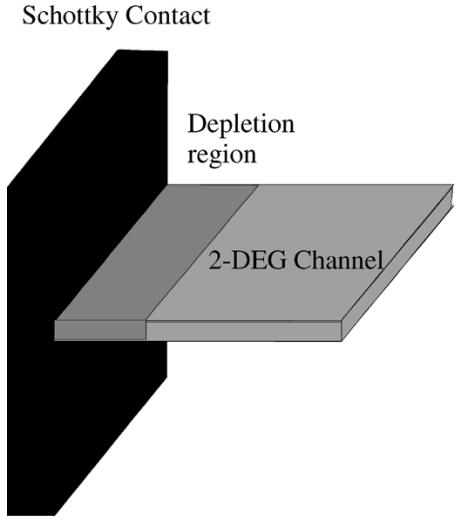

Fig. 1. Schematic view of the 3-D/2-D contact, also showing the depletion region which appears between the metal and the 2-DEG channel. The semicondutor layers above and below the 2-DEG channel are not shown.

Despite the significant amount of device related work, the number of investigations on the modeling of the capacitance–voltage (*C–V*) and current–voltage (*I–V*) characteristics of these metal to 2-DEG interfaces is still limited. In the following section, we develop a novel quasi-2-D model for the *C–V* characteristics, by starting from a self-consistent solution of the Schrödinger and Poisson equations in the growth direction. Next, we investigate the *I–V* characteristics, discussing the behavior of Schottky contacts where the Schottky metal contacts directly the 2-DEG. Our formalism includes both tunneling and thermionic emission mechanisms in an unified fashion, extending most of the previous formulations [4]–[6], which generally address each mechanism separately. The obtained results are contrasted with those for conventional Schottky devices and the expected performance advantages of using low-dimensional Schottky contacts in photodetection applications are highlighted.

II. *C-V* Modeling

The formulations available in the literature to study the *C–V* characteristics of metal to 2-DEG interfaces can be divided into

Manuscript received July 28, 2004; revised November 29, 2004. This work was supported in part by Fapesp, Sao Paulo State Research Foundation, Brazil, under a D.Sc. fellowship, in part by the National Science Foundation under Grant ECS 0117073, and in part by the Nano Technology Institute of the State of Pennsylvania. The review of this paper was arranged by Editor L. Lunardi.

R. Ragi and M. A. Romero are with the Department of Electrical Engineering, University of São Paulo, Sao Carlos, SP 13564-250, Brazil (e-mail: muriloa@sel.eesc.usp.br).

B. Nabet is with the Department of Electrical and Computer Engineering, Drexel University, Philadelphia, PA 19104 USA.

Digital Object Identifier 10.1109/TED.2004.842718

two classes. On one hand, Gelmont and collaborators [7] extended the work by Petrosyan and Shik [4] to obtain, by using the conformal mapping technique, an analytical expression for the junction capacitance between a bulk p-type semiconductor and a 2-DEG. However, their expression becomes progressively less accurate as the contact depth R is made much smaller than the depletion width, as in the limiting case of an ideal metal to 2-DEG junction. Also, changes in the layer structure or the conduction band diagram are accounted for only through the 2-DEG carrier concentration, n_s.

On the other hand, fully numerical techniques are also available. Such implementations use either the boundary element method [8] or the finite-element method [9] for the resolution of the Schrödinger and Poisson equations. Both methods are very time consuming from the computational point of view, but they often do not yield self-consistent solutions. Although the problem of interest here is intrinsically 2-D, due to the presence of the lateral Schottky terminal, usually only the Poisson equation is solved in two dimensions. The Schrödinger equation is still written as a function of the growth direction only.

The novel method proposed here builds on those previous investigations, in an attempt to combine the attractive features of both classes of formulations discussed above. Specifically, in the next section, we use the analytical description proposed by Petrosyan to represent the longitudinal potential $V(x)$ along the 2-DEG channel [4] in order to develop a quasi-2-D extension of the self-consistent Schrödinger-Poisson solver presented by the authors in [10]. In this way, it is possible to explicitly incorporate the layer structure in the formulation. However, the computational effort is much smaller than required by fully numerical techniques [8], [9].

A. Theoretical Formulation

The model presented in this section is a quasi-2-D extension of work previously published by the authors [10]. We start by self-consistently solving Schrödinger and Poisson equations in the growth direction. The quantum–mechanical formalism is based on the effective mass approximation, where the electron wavefunction is taken as the product of a Bloch function and an envelope function, solution of the time-independent Schrödinger equation

$$H\Psi_i(z) = E_i\Psi_i(z) \tag{1}$$

where z is the direction perpendicular to the epitaxial layers. The utilized Hamiltonian is based on a generalized expression suited for both conventional as well as strained quantum-well devices, since it is able to account for position-dependent effective mass and lattice constant. It is given by

$$H = \left[-\frac{\hbar^2}{2a(z)}\frac{d}{dz}\left(\frac{a^2(z)}{m^*(z)}\frac{d}{dz}\frac{1}{a(z)}\right) + V_{\rm ef}(z)\right]$$

where the potential $V_{\rm ef}$ includes not only the band-diagram discontinuities and the Hartree term due to the electrostatic potential but also an exchange-correlation term as well as strain components caused by lattice mismatch [10]. Specifically, the effective potential operator $V_{\rm ef}$ is given as the sum of four terms

$$V_{\rm ef}(z) = V_e(z) + qV(z) + C_1(\varepsilon_{\rm xx} + \varepsilon_{\rm yy} + \varepsilon_{\rm zz}) + V_{\rm xc}(z) \tag{2}$$

where $V_e(z)$ represents the conduction-band edge potential of the undoped structure, i.e., the band-diagram discontinuity, and $V(z)$ is the Hartree term due to the electrostatic potential. For completeness, we have also included an exchange-correlation term $V_{\rm xc}(z)$, while the strain caused by lattice mismatch, if any, can be account for the second term of the right-hand side of (2). In this term, C_1 is the conduction band deformation potential, and $\varepsilon_{\rm xx}$, $\varepsilon_{\rm yy}$, and $\varepsilon_{\rm yy}$ are the strain components [10].

The Poisson equation, which yields the Hartree term, is given by

$$\frac{d}{dz}\left(\varepsilon_0\kappa(z)\frac{d}{dz}\right)V(z) = \frac{-q\left(N_d^+(z) - N_a^-(z) - n(z)\right)}{\epsilon_0} \tag{3}$$

where q is the electronic charge, $\kappa(z)$ is the position dependent dielectric constant of the semiconductor, $N_d^+(z)$ is the ionized donor concentration, $N_a^-(z)$ is the ionized nonintentional background acceptor concentration, and $n(z)$ is the free-electron concentration in the conduction band (the free hole concentration has been neglected). We write $n(z)$, in terms of the electronic eigenfunctions $\Psi_i(z)$, as

$$n(z) = \frac{m^*}{\pi\hbar^2}k_BT\sum_i \ln\left[1 + \exp\left(\frac{(E_F - E_i)}{k_BT}\right)\right]|\Psi_i(z)|^2 \tag{4}$$

where m^* is the electron effective mass in the 2-DEG channel, k_B is the Boltzmann constant, T is the absolute temperature, $\hbar$ is the reduced Planck constant, E_F is the Fermi-level energy, and E_i represents the ith eigenvalue. Summation is carried out over all i subbands.

The ionized donor concentration $N_d^+(z)$ is described by

$$N_d^+(z) = \frac{N_d(z)}{1 + g.e^{\frac{(E_F - E_d)}{kT}}} \tag{5}$$

where $N_d(z)$ is the position-dependent donor concentration, g is the donor level spin degeneracy factor, taken as equal to 2, and E_d is donor ionization energy.

The Fermi-level position E_F is computed from the usual charge neutrality condition in the bulk material, and the above formulation (1)–(5) must be solved self-consistently in real space. In particular, the eigenstates of the Schrödinger equation are numerically calculated by using a split-operator algorithm through a nonuniform finite-difference discretization scheme [10], under the boundary conditions that the wavefunction must vanish at the substrate and at the device top surface. The boundary conditions for the Poisson equation are given by the surface potential V_s at the top of the device (taken as $z = 0$) as well as by the position of the conduction band with respect to the Fermi-level in the bulk semiconductor, presenting a nonintentional background ionized doping density N_A^-.

The solution yields the charge control relation between the surface potential V_s, which is the surface potential on the AlGaAs layer in the absence of a gate contact, and the sheet electron density n_s into the channel. Now, this charge control relation is used as an input to develop a quasi-2-D model for the *C–V* characteristics of metal to 2-DEG junctions.

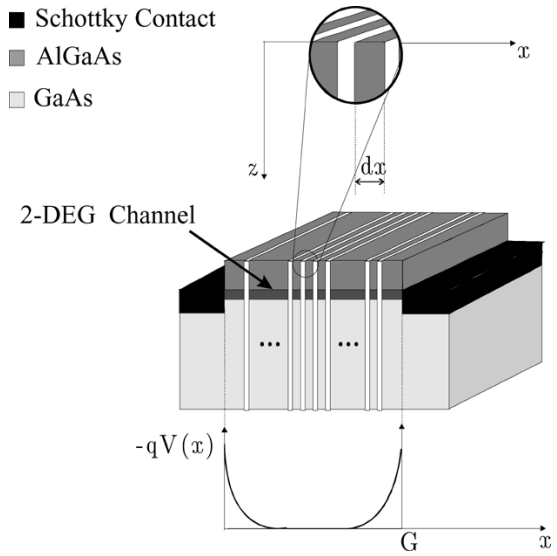

Fig. 2. Schematic view of the geometry and associated calculation procedure for the *C–V* characteristics. The lateral Schottky contacts, in black, directly contacting the 2-DEG channel, are the same indicated in Fig. 1. On the top of the device a surface potential is assumed, which is the surface potential on the top of the AlGaAs layer in the absence of the usual gate electrode of a HEMT device.

B. Two-Dimensional Extension and Results

In the framework outlined previously, if the sheet electron density n_s into the 2-DEG channel is obtained above as a function of the surface potential V_s, i.e., $n_s = f(V_s)$, then the x-component of the potential distribution along the channel $V(x)$ can be taken into account assuming, as usually done in the modeling of other 2-DEG-based devices [11], [12], assuming that $n_s(x) = f(V_s - V(x))$, preserves the same functional dependence.

Therefore, according with our procedure, schematically depicted in Fig. 2, for a given terminal voltage applied to the Schottky contact V_T, the channel is initially divided into several segments of width dx. Next, the capacitance contribution of each segment is computed by solving the unidimensional Schrödinger–Poisson problem in the growth direction, but now under an "effective" surface potential $V_s' = V_s - V(x_i)$, where x_i is a coordinate position the located in middle of each segment dx. A quasi-static approach was used, giving the capacitance per unit area as the total charge variation caused by a small voltage change around a given bias point. Then, the capacitance component due to the free carriers C_{free} is given by the summation of the capacitance contribution for each segment dx.

We have previously published a preliminary theoretical analysis, which served as guideline for device optimization [13]. Here, we conduct a much more detailed model validation, comparing our results with the experimental data provided by Shur and coworkers [2]. Their layer sequence is given as follows: on top of a semi-insulating GaAs substrate 20 000 Å of 2×10^{14} cm^{-3} GaAs buffer layer were deposited, followed by a 30-Å undoped $Al_{27}Ga_{73}As$ spacer layer and 300 Å of 1.5×10^{18} cm^{-3} doped n-type $Al_{27}Ga_{73}As$ supply layer. The topmost layer is a 200-Å cap layer. All growth was done by molecular beam epitaxy, and total device area is 1.5×40 μm.

It should be noted that independently of the physical mechanism responsible for charge modulation by the applied bias, if the voltage is high enough to fully deplete the semiconductor, the capacitance between the electrodes will reach a strictly geometrical lower value C_g related to the configuration of the electrodes as well as to the dielectric constant of the semiconductor material. Therefore, the overall capacitance is given by the contribution of two terms. In what follows, the geometrical value is already extracted from the experimental data, and the discussion is concerned only with the free electron contribution C_{free} to the device capacitance.

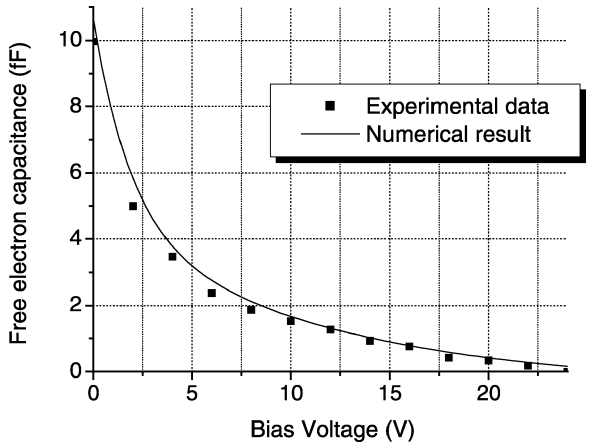

Fig. 3. Theoretical predictions (solid lines) and experimental data (dots) for the free carrier capacitance of the HEMVAR device.

Thus, in our computational procedure, to obtain the theoretical results we used the method described above, employing the Petrosyan approximation for the longitudinal potential $V(x)$ [4]

$$V(x) = \frac{qn_{s_0}}{2\pi\epsilon}\left(x \ln \frac{\sqrt{d_{dp}^2 - x^2} + d_{dp}}{\sqrt{d_{dp}^2 - x^2} - d_{dp}} + 2d_{dp} arc\sin \frac{x}{d_{dp}}\right) \tag{6}$$

where q is the electon charge, n_{s_0} is the density of 2-DEG, in equilibrium, d_{dp} is the depletion region in the metal to 2-DEG juntion (see Fig. 1), and ϵ is the dielectric constant of the GaAs.

We simulated exactly the same layer structure discussed previously and calibrated the surface potential V_s, due to surface states causing Fermi-level pinning at the semiconductor/air interface, in such way that our quantum-mechanical simulator yielded the measured value of 8×10^{11} cm^{-2} for the 2-DEG carrier concentration [2]. Therefore, the only unknown parameter is the height of the Schottky barrier contacting the 2-DEG channel, taken here as 0.8 eV. Even using no fitting parameters, the agreement between our theoretical predictions and the experimental findings of [2] can be considered to be quite satisfactory. In fact, as indicated Fig. 3 and Table I, both results are very close, and the relative error increases only for high values of bias voltages, when the measured capacitance is very small.

III. *I–V* Characteristics

In this section, we develop a model for the *I–V* characteristics of metal to 2-DEG contacts. Unlike most of the previous formulations [4]–[6], we made an effort to address both tunneling and thermionic emission in a unified fashion. Therefore, in this more general framework, the carrier transport across the

TABLE I
EXPERIMENTAL (EXP) AND THEORETICAL (NUM) *C–V* CHARACTERISTICS FOR THE HEMVAR DEVICE. THE RELATIVE ERROR IS ALSO SHOWN

Voltage (V)	*C(fF) exp.*	*C(fF) num.*	*Relative Error (%)*
0	9,96	10,43	4,81
2	4,99	5,73	14,89
4	3,47	3,80	9,53
6	2,37	2,77	17,22
8	1,86	2,11	13,65
10	1,52	1,64	8,48
12	1,27	1,31	3,78
14	0,93	1,04	12,87
16	0,76	0,75	0,93
18	0,42	0,60	44,69
20	0,34	0,47	40,91

metal—2-DEG interface is characterized by the quantum-mechanical transmission coefficient (T), defined as the ratio of the transmitted to the incident current. Carriers can traverse from the 2-DEG to the metal and vice-versa, corresponding to current densities designated by $J_{g\to m}$ and $J_{m\to g}$, respectively. The expression for $J_{g\to m}$, for a parabolic energy-momentum relation, is proportional to the transmission coefficient $T(E_x)$ multiplied by the occupation probability in the 2-DEG, $f_g(E)$, the Fermi-Dirac distribution function in the gas, and the unoccupied probability in the metal, $1-f_m(E)$

$$J_{g\to m}=q\frac{2}{h^2}\int T(E_x)f_g(E)\left[1-f_m(E)\right]\frac{\partial E}{\partial p_x}dp_x dp_y \quad (7)$$

where h is the Planck's constant, q is the electron charge, E is the electron energy, $\partial E/\partial p_x$ is the electron velocity in the x-direction, p_y is the electron moment component normal to the direction of the current flow, and E_x is the carrier kinetic energy in the x-direction. $T(E_x)$ is the probability that an electron with energy E_x will pass through the barrier, which can be determined by the WKB approximation [14], described by the following semiclassical expression:

$$T(E_x)=\exp\left[-\frac{2}{\hbar}\sqrt{2m}\int\left(\sqrt{qV(x)+E}\right)dx\right]$$

where $qV(x)$, given by (6), is the potential energy barrier for an electron within the depletion region of a heterodimensional metal–2-DEG system.

It is worth mentioning that the arguments used to construct (7), the same starting point chosen by Tait [15], are essentially the same developed when the tunneling phenomena between solid conductors was first studied by Frenkel [16]. However, due to the low-dimensional nature of the 2-DEG, the electron motion is confined to the quantum well at the $Al_xGa_{1-x}As$–GaAs interface, where the first available energy state is above the conduction band by the amount of the first confined state E_0. Based on this boundary condition, the equation above was obtained by restricting ourselves to the case where that the electron population is low enough so that only the first energy level of the 2-DEG presents a significant carrier concentration.

Then, treating the potential barrier as 1-D, so that the transmission probability $T(E_x)$ can be written in terms of only one dimension, and considering that the tangential component of electron momentum is conserved during the transition metal–semiconductor [17], E_x can be replaced by $E-E_\perp-E_0$, where $E_\perp=(p_y^2)/2m^*[dp_y=(m^*/(2E_\perp))^{1/2}dE_\perp]$ represents the component of energy associated with the direction parallel to the barrier, y direction. The integration over p_x can be carried out over the variable E, due to the presence of the velocity factor $\partial E/\partial p_x$ in (7), while the integration over p_y can be performed by relating p_y to $E_\perp$, so that (7) becomes

$$J_{g\to m}=q\frac{2}{h^2}\left(\frac{m^*}{2}\right)^{\frac{1}{2}}\int_{E_0}^{\infty}f_g(E)\left[1-f_m(E)\right]dE \times\int_0^{E-E_0}T(E-E_\perp-E_0)E_\perp^{-\frac{1}{2}}dE_\perp. \quad (8)$$

The net current is now obtained by taking into account the two components flowing in opposite directions

$$\begin{aligned}J&=J_{g\to m}-J_{m\to g}\\&=\frac{q\sqrt{2m^*}}{h^2}\int_{E_0}^{\infty}\left[f_g(E)-f_m(E)\right]\times\left\{\int_0^{E-E_0}T(E-E_\perp-E_0)(E_\perp)^{-\frac{1}{2}}dE_\perp\right\}dE. \quad (9)\end{aligned}$$

The above equation is a unified and general expression valid for all energy range. In the next subsection, we obtain a analytical expression to the limiting case where the thermionic emission is the dominant transport process.

A. Thermionic Emission

Restricting ourselves to the case where the velocity of incident carriers is greater than the minimum velocity v_{0_x}, corresponding to the threshold energy above built-in-potential, with $m^*v_{0_x}/2=q(V_{bi}-V)$, in the high-temperature range where the Fermi statistics reduces to the Boltzmann statistics, the Fermi distribution can be written as $f_g(E)=\exp[-(E-E_F-qV)/k_BT]$. After some approximations, such as $T(E-E_\perp)\simeq 1$ and $f_m(E)\approx 0$, in (7), (8) becomes

$$J_{g\to m}=q\frac{2}{h^2}\left(\frac{m^*}{2}\right)^{\frac{1}{2}}\times\int_{E_0+\frac{m^*v_{0_x}}{2}}^{\infty}\exp\left[-\frac{(E-E_F-qV)}{k_BT}\right]dE\times\int_0^{E-E_0}E_\perp^{-\frac{1}{2}}dE_\perp.$$

Changing coordinates once again and using the same mathematical manipulations performed previously, we write

$$J_{g\to m}=q\frac{2}{m^*h^2}\exp\left[\frac{-(E_0-E_F-qV)}{k_BT}\right]\times\int_{m^*v_{0_x}}^{\infty}\exp\left[-\frac{E_x}{k_BT}\right]p_x dp_x\times\int_0^{\infty}\exp\left[-\frac{E_\perp}{k_BT}\right]dp_y$$

with $E = mv_x^2/2 + mv_y^2/2 + E_0 + q(V_n + V)$, where $qV_n = E_C - E_F$. The current density results

$$J_{g\to m} = \frac{2q}{h^2}\sqrt{2\pi m^*}(k_BT)^{\frac{3}{2}} \times \exp\left(-\frac{E_0}{k_BT}\right)\exp\left(-\frac{q\phi_B}{k_BT}\right)\exp\left(\frac{qV}{k_BT}\right) \quad (10)$$

where $q\phi_B = q(V_{b_i} + V_n)$.

Equation (10) yields the current density traversing a metal-2-DEG interface due to electron flow from the 2-DEG to the metal in the thermionic approximation framework. The complete expression for the current density can be obtained considering that, in equilibrium, $J_{g\to m}$ equals $J_{m\to g}$. Thus, $J_{m\to g}$ can be found by

$$J_{m\to g} = -J_{g\to m}(V = 0).$$

The net current density is finally given by

$$J = \frac{2q}{h^2}\sqrt{2\pi m^*}(k_BT)^{\frac{3}{2}} \times \exp\left(-\frac{E_0}{k_BT}\right) \times \exp\left(-\frac{q\phi_B}{k_BT}\right)\left[\exp\left(\frac{qV}{k_BT}\right) - 1\right]. \quad (11)$$

Equation (11) resembles the result obtained for a standard Schottky contact, according to Bethe in his seminal work [18]. However, it should be stressed that the term in E_0, the energy of the first confined state, is not a phenomenological factor but rather arises directly from the derivation. Independent experimental evidence of this barrier enhancement effect due to energy level quantization was already provided in [19].

Comparing the results yielded by the complete formulation (7) and the thermionic approximation (11), our simulations indicate that both equations produce essentially the same results at room temperature, demonstrating that electron transport is dominated by thermionic emission. However, for low-temperature cryogenic operation, the tunneling component starts to become significant and must be accounted for, in particular for high values of 2-DEG carrier density, approaching 10^{12} cm^{-2}.

B. Thermionic Emission Current: Comparison to Conventional Schottky Contacts

As discussed above, essential differences do exist between the transition from a bulk metal to a bulk semiconductor versus the transition from a bulk metal into a 2-D system. From the device-level point of view, the effect of the first confined state E_0 emerging from (11) is to produce an exponential reduction of the reverse saturation current by an increase in the effective Schottky barrier height. The ratio for the saturation currents in both systems, can be obtained from (11) and by the well-known expression for the saturation current in a conventional Schottky contact, as given by the Dushmann–Richardson equation. One can show that

$$r = \frac{I_{3-D}}{I_{2-D}} = \frac{L}{h}\sqrt{2\pi m^* kT}\exp\left(\frac{E_0}{kT}\right) \quad (12)$$

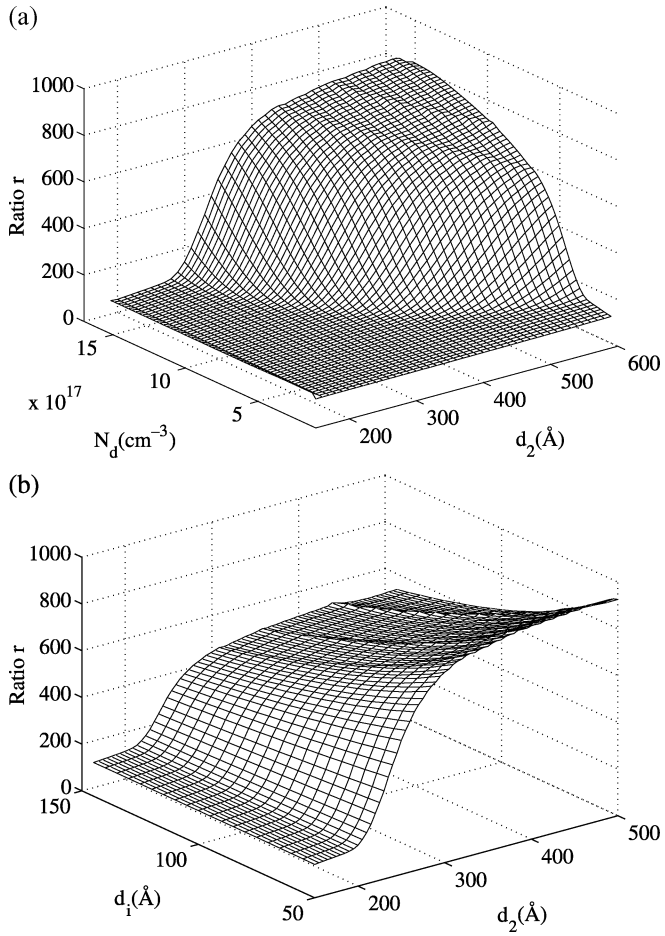

Fig. 4. Ratio of thermionic emission currents for conventional and metal to 2-DEG Schottky contacts, as function of (a) doping level N_d and thickness d_2 of the layer AlGaAs and (b) thickness d_2 of the layer AlGaAs and thickness d_i of the undoped AlGaAs spacer layer. The parameter L was taken as 1.0 μm.

where L is associated to the contact geometry and E_0, the position of the first energy level, which can be readily calculated by using the quantum–mechanical formalism previously described in Section II.

The behavior of the ratio r between the thermionic emission for conventional and $Al_{24}Ga_{76}As$-GaAs Schottky contacts, as a function of the doping level, the thickness of the $Al_{24}Ga_{76}As$ layer and the thickness of the $Al_{24}Ga_{76}As$ undoped spacer layer is shown in Fig. 4(a) and (b). The large values achieved represent a strong suppression of thermionic emission current, essentially due to the exponential term in E_0. This term acts as an effective Schottky barrier enhancement due to energy quantization. By itself, this feature certainly makes these structures very attractive as low-noise photodetectors as well in low-leakage gate contacts.

There are fabrication issues still to be solved concerning the fabrication of high-quality metal to 2-DEG contacts, in order to completely eliminate the current flow through the adjacent semiconductor layers. However, our experimental data, shown in Fig. 5 where we compare the two metal–semiconductor–metal (MSM) photodetectors with identical layer structures, one of them employing metal to 2-DEG Schottky contacts, shows that effective dark current reduction, by almost

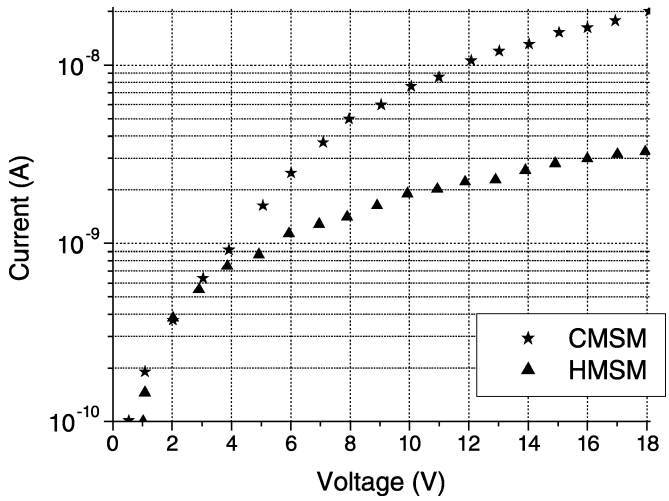

Fig. 5. Dark current characteristics of two MSM photodetectors employing identical layer structure. The device labeled CMSM uses conventional Schottly contacts, while the device labeled HMSM uses metal to 2-DEG contacts.

one order of magnitude, was achieved, in fair agreement to our theoretical expectations.

IV. Conclusion

In this paper, we focused our interest in devices based on the contact between a metal and a 2-DEG. A model for the *C–V* characteristics was implemented and validated by comparison to reported experimental data. A novel model for the *I-V* characteristics, considering both tunneling and thermionic emission mechanism. was also developed. The model suggests that such contacts can be very attractive for the fabrication of ultralow-noise Schottky or MSM photodetectors.

References

[1] H. Okada, K. Jinushi, N. J. Wu, T. Hashizume, and H. Hasegawa, "Novel wire transistor structure with in-plane gate using direct Schottky contacts to 2-DEG," *Jpn. J. Appl. Phys.*, vol. 34, no. 2B, pp. 1315–1319, Feb. 1995.

[2] W. C. Peatman, T. W. Crowe, and M. Shur, "Design and fabrication of heterostructure varactor diodes for millimeter and submillimeter wave multiplier applications," in *Proc. IEEE/Cornell Conf. Advanced Concepts High Speed Semiconductor Devices Circuits*, Ithaca, NY, 1991.

[3] M. S. Shur, W. C. Peatman, H. Park, W. Grimm, and M. Hurt, "Novel heterodimensional diodes and transistors," *Solid State Electron.*, vol. 38, no. 9, pp. 1727–1730, Sep. 1995.

[4] S. G. Petrosyan and A. Y. Shik, "Contact phenomena in a 2-DEG," *Sov. Phys. Semiconduct.*, vol. 23, no. 6, pp. 696–697, Jun. 1989.

[5] A. Anwar, B. Nabet, J. Culp, and F. Castro, "Effects on electron confinement on thermionic emission current in a modulation doped heterostructure," *J. Appl. Phys.*, vol. 85, no. 5, pp. 2663–2666, Mar. 1999.

[6] L. V. Asryan, S. G. Petrosyan, and A. Y. Shik, "Tunnel current across a contact with a 2-DEG," *Sov. Phys. Semiconduct.*, vol. 24, no. 12, pp. 1316–1318, Dec. 1990.

[7] B. Gelmont, M. Shur, and C. Moglestue, "Theory of junction between 2-DEG and p-type semiconductor," *IEEE Trans. Electron Devices*, vol. 39, no. 5, pp. 1216–1222, May 1992.

[8] Y. C. Luo, S. J. Wang, Y. G. Chiou, J. C. Lin, and C. Y. Cheng, "Two-dimensional numerical simulation of Si Schottky/2-DEG barrier diode using boundary element method," *Jpn J. Appl. Phys.*, vol. 34, no. 10, pp. 5556–5561, May 1995.

[9] Silvaco International, ATLAS—Device Simulation Software, Santa Clara, CA, 1998.

[10] J. E. Manzoli, M. A. Romero, and O. Hipólito, "On the capacitance-voltage modeling of strained quantum-well MODFETs," *IEEE J. Quantum Electron.*, vol. 34, no. 12, pp. 2314–2320, Dec. 1998.

[11] H. Rohdin and P. Roblin, "A MODFET DC model with improved pinchoff and saturation characteristics," *IEEE Trans. Electron Devices*, vol. 33, no. 5, pp. 664–672, May 1986.

[12] K. Lee, M. Shur, T. J. Drummond, and H. Morkoç, "Current-voltage and capacitance-voltage characteristics of modulation-doped field effect transistors," *IEEE Trans. Electron Devices*, vol. 30, no. 3, pp. 207–212, Mar. 1983.

[13] A. Anwar, B. Nabet, R. Ragi, J. E. Manzoli, and M. A. Romero, "Gate controlled 2-DEG varactor for VCO applications in microwave circuits," *Microelectron. J.*, vol. 33, no. 5–6, pp. 495–500, May 2002.

[14] F. A. Padovani and R. Stratton, "The accuracy of the WKB approximation for tunneling in metal-semiconductor junctions," *Appl. Phys. Lett.*, vol. 13, no. 5, pp. 167–169, May 1968.

[15] G. B. Tait and B. Nabet, "Current transport modeling in quantum-barrier-enhanced heterodimensional contacts," *IEEE Trans. Electron Devices*, vol. 50, no. 12, pp. 2573–2578, Dec. 2003.

[16] J. Frenkel, "On the electrical resistance of contacts between solid conductors," *Phys. Rev.*, vol. 36, pp. 1604–1618, Dec. 1930.

[17] R. Stratton, "Theory of field emission from semiconductors," *Phys. Rev.*, vol. 125, no. 1, pp. 67–82, Jan. 1962.

[18] H. A. Bethe, "Theory of the boundary layer of crystal rectifiers," MIT, Cambridge, MA, MIT Radiation Lab. Rep., 1942.

[19] T. Ytterdal, M. S. Shur, M. Hurt, and W. C. B. Peatman, "Enhancement of Schottky barrier height in heterodimensional metal-semiconductor contacts," *Appl. Phys. Lett.*, vol. 70, no. 4, pp. 441–442, Jan. 1997.

Regiane Ragi was born in Mogi das Cruzes, Brazil, in 1968. She received the B.Sc., M.Sc., and D.Sc. degrees from the Physics Institute of the University of São Paulo, São Paulo, Brazil, in 1994, 1997, and 2003, respectively.

She is currently a Postdoctoral Fellow working on solid-state and nanoelectronic devices with the Electrical Engineering Department, University of São Paulo, São Carlos.

Murilo Araujo Romero was born in Rio de Janeiro, Brazil, in 1965. He received the B.Sc. and M.Sc. degrees, both in electrical engineering, from Pontifical Catholic University, Rio de Janeiro, Brazil, in 1988 and 1991, respectively, and the Ph.D. degree from Drexel University, Philadelphia, PA, in 1995.

He is now an Associate Professor of electrical engineering at the University of São Paulo, São Carlos, Brazil. He has published more than 50 papers in conferences and journals, including the IEEE Transactions on Electron Devices, IEEE Transactions on Microwave Theory and Techniques, IEEE Journal of Quantum Electronics, and IEEE Photonics Technology Letters. His current research interests are focused on optical fibers and optical communications as well as on the modeling and simulation of semiconductor devices and circuits.

Bahram Nabet (M'00) received the B.S.E.E. degree with honors from Purdue University, West Lafayette, IN, in 1977, and the M.S.E.E. and Ph.D. degrees from the University of Washington, Seattle, in 1985 and 1989, respectively.

He joined the faculty of Drexel University, Philadelphia, PA, in 1989, where he is presently a Professor of electronics and computer engineering and Associate Dean for Special Projects in the College of Engineering. His areas of research include semiconductor devices, optoelectronics, reduced-dimensional systems, and fiber optic networks and devices. He is coauthor of two books and over 100 refereed publications. He has been a Senior Visiting Scientist in Brazil and Italy and was on sabbatical leave from Telcordia Applied Research, Inc.

Dr. Nabet has won six Best Professor teaching awards from students as well as a departmental and a university-wide teaching award. He is a member of AAAS, AAHE, and HKN.